Multiregime MEMS Sensor Networks for Smart Structures

S.C. Jacobsen* [a], B.J. Maclean[a], M. Whitaker[a], M. Olivier[a] and M.G. Mladejovsky[b]

[a]Sarcos Research Corporation, 360 Wakara Way, Salt Lake, Utah 84108

[b]Center for Engineering Design, University of Utah, Salt Lake UT 84112.

ABSTRACT

This paper discusses sensor IC design and packaging approaches, sensor networks architecture and communication protocols, as well as current and future applications of a series of transducers which we have developed in order to address several of the unmet needs of sensing and closed loop control of smart structures and organism-like machines of the future. In particular, the approach described therein has been used to design and manufacture sensors tailored for the measurement of strain, rotation, displacement, pressure, vibration, flow, multi-axis fluid shear, multi-axis strain, touch, multi-axis acceleration, and sound. This paper describes a suite of networkable sensors designed to monitor the internal state of a system, such as strain and joint angle, as well as that of the environment and contact interface with the system, such as pressure, shear stress and contact forces and moments.

Keywords: MEMS, Sensors, Sensor Networks, Pressure, Strain, Rotation, Vibration, Shear Flow, Multi-Axis Strain.

1. INTRODUCTION

Sarcos Research Corporation (SRC) has focused efforts on the development of servo controlled machines such as high performance robots and telerobotic systems, mobility interfaces for synthetic environments, artificial arms, pumps for precise drug delivery and many others systems ranging from 80,000 lbs robotic machines (Jurassic Park figures) to 1 cubic millimeter devices for the administration of drugs. These systems and other smart structures have a common characteristics of being sensor, actuator and control intensive. For example, one robotics project for Euro-Disney used thousands of high resolution rotation and strain sensors for the closed-loop motion and impedance control. A typical robot included 50 Degrees-of-Freedom (DOF) and required approximately 90 sensors and 50 actuators. Figure 1 illustrates this point by showing typical interactions and information that must be processed by such systems.

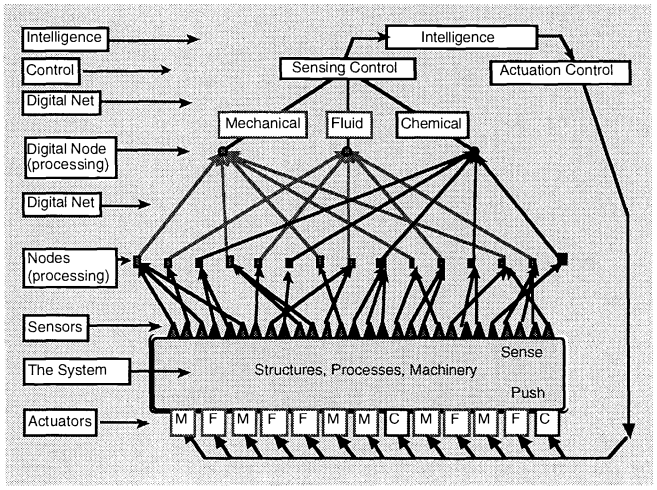

Figure 1: Block diagram illustrating sensor data path, decision layers, and control typically used in smart structures, process control and servo controlled machinery.

While developing these systems the team from SRC encountered a recurring problem, that of high cost and poor reliability of sensors and wiring harnesses. For instance, entertainment robotics projects alone have required over 4000 sensors and 2000 actuators. In these applications, sensors have accounted for up to 30 percent of system cost, and up to half of the system failures have occurred in the supporting wiring harnesses and connectors. Sensors and wiring assemblies have been primary drivers of cost and reliability in other similar applications such as undersea tele-robots, prosthetic limbs, and body motion capture systems (where wiring is routed across moving structures and sensors reside in harsh environments). Yet, in order to even begin to emulate some of the exquisite characteristics of living organisms, such as control, health monitoring, and failure detection in real time, these systems and future smart structures will increasingly rely on sensor-intensive "intelligent" closed-loop control of large arrays of actuators and effectors as illustrated in Fig. 1.

In order to fill this gap SRC began, in the early 80's, to investigate new approaches for reliable and economically viable sensor and network designs[1-6]. Specifically required were robust systems with: high resolution, absolute digital multiplexed output, small size, and low cost. Of main interest were the multiplexed systems which could reduce the wire counts necessary to support interconnected groups of multi-regime sensors.

* Corresponding author: Email: s.jacobsen@sarcos.com; Telephone: 801-581-0155; Fax: 801-581-1151

Discussions initiated in 1985 led, in 1986, to a first proposal to DARPA "Micro Electro Mechanical Systems" (MEMS). In that project, and later others as well as those currently funded by DARPA, NASA, NAVSEA, and commercial sponsors, a number of approaches have been investigated. These efforts have resulted in the development of a new generation of strain, rotation, multi-axis load, shear stress, pressure, vibration and other sensors. Some of these sensors are now emerging from those development efforts and are now a part of preliminary application efforts in aircraft (F18, F15, C141, C130), helicopters (AH-64 and UH-60), submarines (LSV, RCM), operation monitoring systems for rolling assets, robots, automotive, and structural systems. It is anticipated that these sensors will be used in applications ranging from structure prognostics and health monitoring, closed-loop control of flow around hydrodynamic surfaces, sound reduction, and others. The general design approach as well as current and future applications are discussed in the following sections.

2. SUBSYSTEMS

The development of high performance, reliable and economically viable sensor networks for smart structures and systems is a complex problem that involves optimization of IC chips, packaging methods, network architecture and built-in "intelligence" in the form of local control loops, data filtering and storage, self tests and calibration, low power modes and others. The following sections provide an overview of how we have, so far, addressed some of these issues.

2.1 MEMS Transducers - Integrated Circuit Approach

The sensors discussed in this paper are composed of two basic subsystems - (1) a planar silicon base which contains an array of field detectors along with supporting electronics, and (2) a companion array of electrostatic field emitters residing on the surface of an adjacent planar armature made of quartz, sapphire, or glass. Base and armature surfaces interact in close proximity and can, depending on the configuration of emitter and detector arrays, measure specified relative movements between the armature and base with high resolution. Figure 2 is a schematic representation of a typical field detector consisting of an integrating charge amplifier coupled to an array of field emitters. Figure 3 shows the armature and base used in one version of the Rotational Displacement Transducer (RDT).

In all devices we have built to date, the gap between armature and base is small and is tightly maintained either by direct contact, between bearing surfaces created on the structures, or by a suspension system composed of adjacent bearings or flexures. In the examples of this paper, relative movements range from one to six Degrees Of Freedom (DOF).

Emitters and detectors which reside on armatures and bases are the fundamental measuring elements in each sensor. A detector (typically 20 to 150 by 50 to 150 μm) is a conductive region on the base which is connected to a local circuit that performs amplification and conversion functions. An emitter (typically 30 to 200 by 100 to 300 μm) is a conductive region on the armature which is driven either capacitively from the base, or by a connected source. The shape details of emitters and detectors varies significantly for different sensors.

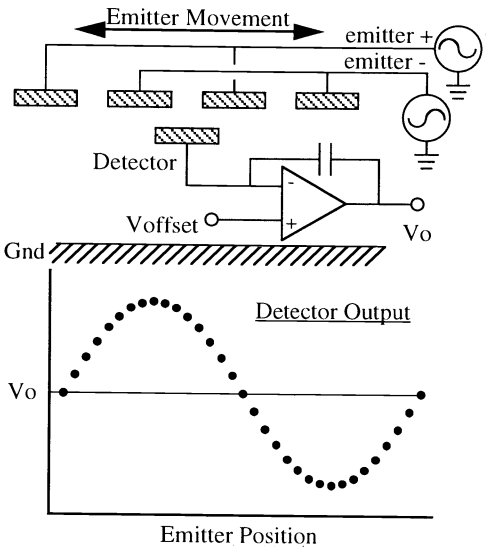

Figure 2: Schematic diagram showing bipolar emitters, single detector and associated circuitry. The detector output signal is shown in the lower diagram as a function of the lateral position of the emitter (armature).

Emitters and detectors are configured into arrays designed to be maximally sensitive to certain relative motions between base and armature, and minimally sensitive to other movements. Onto the emitter array is impressed one or a group of signals which are then sensed by the detector array. Figure 4 schematically illustrates one simple arrangement of emitters, detectors, and circuits configured linearly with slightly different spacing to form a vernier arrangement. This type of arrangement along with the charge amplifier illustrated in Fig. 2 are used in the UniAxial Strain Transducer (UAST). The output signal produced by such an array of detectors driven by two sets of interleaved emitters and identical inverted waveforms (180 degrees out of phase) is also shown therein at a fixed position of the armature. Note the beats in the interference pattern created by the overlay of the emitter and the detector array.

In the case shown in Fig. 4, the waveform, defined by plotting detector output against its spatial position, resembles a sinusoid. The relative position between the base and the armature is encoded in the phase of this waveform. In general, signals from the detector array are combined by local circuitry and processed to produce a digital signal which represents the relative position of base and armature. Digital signals are created by circuits on the base which operate very uniformly from detector to detector, are drift-free, and can be multiplexed onto a minimal-wire bus using various architectures as discussed in Section 2.3.

Each sensor uses a "front end" which interacts with the physical environment to transform a measured parameter, such as rotation, strain, shear, or pressure, into a micro-movement of the armature which is then converted to a signal by the base chip. Sensors include packages with pass-through mechanisms, or ports, which allow sealed interaction with the environment through the front-end and into the armature. Packages also include sealed conduits to pass wiring between individual sensor nodes and central processing modules (see Section 2.2).

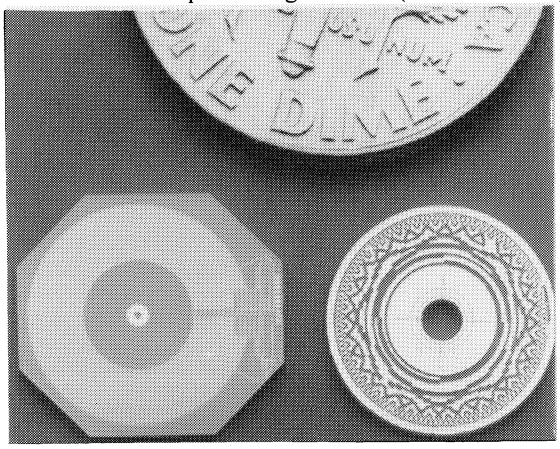

Figure 3: Photograph showing the base and armature used in the rotary displacement transducer (RDT).

Challenges of this approach include: defining array architectures and signal processing schemes for each application, designing base chips with non-standard configurations of circuitry (e.g. non-orthogonal), creating suspension and/or on-chip bearing systems to maintain precise relationships between armatures and bases, defining multiplexing schemes which can be used successfully with existing systems, and designing packages with non-restrictive pass-throughs which are resistant to challenging environments.

2.1.1 UniAxial Strain Transducer Base and Armature

The power and versatility of this approach is well illustrated by examining devices and networks which we have implemented in this way. For instance, the UAST can be integrated as part of a strain sensing network ideally suited for applications such as: condition-based operation and maintenance, integrated load cells, large dynamic range scales, and others[1,2]. Its characteristics include: (1) high resolution, (2) high strain operating range with high allowable overextension without damage (bangs), (3) refresh rates necessary for structural monitoring at lower frequency ranges (up to 1 kHz) and higher ranges for vibration monitoring (up to 20 kHz), (4) system architectures designed for use in excess of 128 sensors on a digital network, (5) high vibration and impact tolerance for rugged applications, (6) shielding against electromagnetic fields, and (7) a package size and shape suitable for a broad range of uses.

Figure 5 shows the major functional blocks implemented onto version 3 of the UAST (UAST 3) IC chip. As indicated earlier, the strain information is obtained by measuring the relative displacement between the base and the armature. The vernier arrangement between the emitter fingers and the detector array results in a quasi-sinusoidal waveform of detector output (see Fig. 4) in which the magnitude of the strain is encoded in the phase of the waveform. To convert the output of 64 detectors into a single digital multiplexed output the following procedure is accomplished on the single chip shown in Fig. 5. First, a series of up to 16 strobe pulses are applied to the emitter fingers in order to record the waveform on the array of 64 charge-integrating amplifiers connected to the detectors. Next, the analog outputs of the detector array are fed to 8 parallel sigma-delta analog-to-digital converters (ADC) which share the task of digitizing the 64 detector values and placing the results in RAM. Each conversion requires $2^{(n+1)}$ clock pulses to create n-bits of detector resolution (supporting from 7 to 12 bits of conversion, depending on the UAST resolution mode selected). To start the strain computation algorithm, a 14-bit triangular waveform of 64 template values is generated with the same period as the detector data but with one of 2^{15} (32,768) phase positions. A convolution can then be performed by successively summing the products between the respective detector and template values at a given template position. When this is done for all 32,768 possible template locations, a periodic function is created whose phase corresponds to the relative position of the armature and base. For efficiency, the convolution is calculated only 15 times by executing a binary search to find the zero-axis crossing of the convolution waveform (this approach yields 15-bits of resolution between the armature and base when operating the ADCs with 12-bit conversions, i.e., 0.35 micro-strain for a 10 mm gage length).

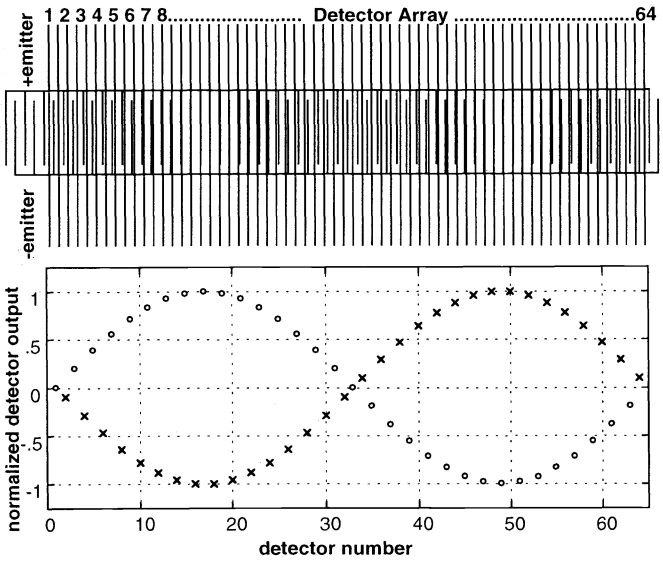

Figure 4: Schematic Representation of UAST emitter fingers and detector array. The space between the emitter fingers and the detectors differs slightly in such a way as to form a vernier pattern. The response of such a detector array for a fixed position of the armature resemble a sinusoid.

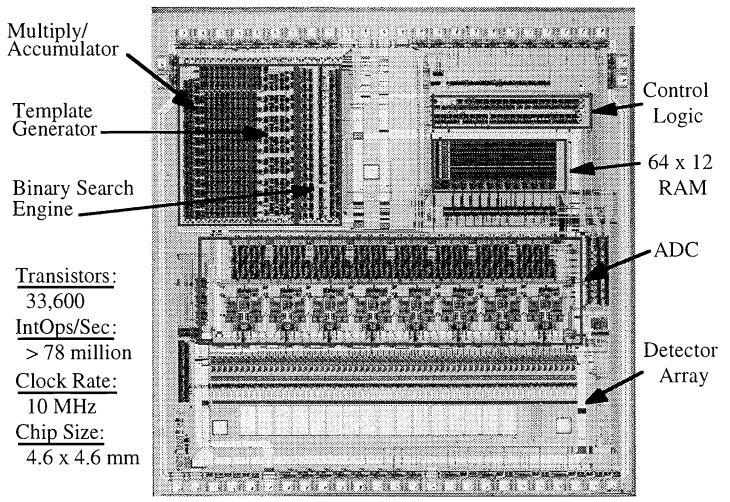

Figure 5: Photograph showing the UAST3 IC chip and its integrated functional blocks

All 64 detector values contribute to the final calculated strain (displacement) value, providing a robust form of spatial filtering which, incidentally, has no sensitivity to DC offsets in the detector waveform and minimizes the influence of vertical displacement of the base with respect to the emitter on the output value. Finally, the resulting digital strain number is multiplexed onto a common 5-wire bus (including power, ground, distributed 10 MHz clock, token, and data) using the token passing method described later in this paper.

An emerging development, the IC chip for UAST 5, will be designed in 0.6 micron CMOS and will include both intrinsic and computation-based temperature compensation, load cycle counting, new strain computation algorithm, power saving auto-sleep modes, high sample rates, smaller foot print, and multiple communication protocols.

2.1.2 BiAxial Strain Transducer (BiAST)

The UAST concept and IC chip architecture has recently been extended to create the BiAxial Strain Transducer (BiAST) as shown in Figure 6. This IC chip is currently at the heart of a two-axis flush mounted, floating element, surface shear stress sensor (which is described in Section 2) and will also be packaged as a multi-axis strain sensor for structural measurements. Similarly to the UAST, the BiAST is a micro-extensometer, not a strain transducer (the sensor base or armature are not distorted but, rather, sensor output is based on measured displacements between the base and armature). As illustrated in Fig. 6 the BiAST base chip includes two orthogonal sets of 64-element detector arrays interacting with a suitably designed set of orthogonal emitter arrays. Together these form two separate verniers which can be used to make measurements for the two in-plane axes. The detector and emitter element spacing are the same as those for the UAST 3. The BiAST also shares the eight analog-to-digital converters, template generator, and strain computation engine of the UAST 3 between the two arrays. As such, the BiAST first samples both detector arrays and then begins conversion of the X-axis detectors with subsequent calculation of the X-axis displacement. The Y-axis detector values are then converted with subsequent calculation of the Y-axis value. Thus, the BiAST can sample only half as fast as the UAST for the same level of output resolution. Otherwise, its performance is on par with that of UAST 3.

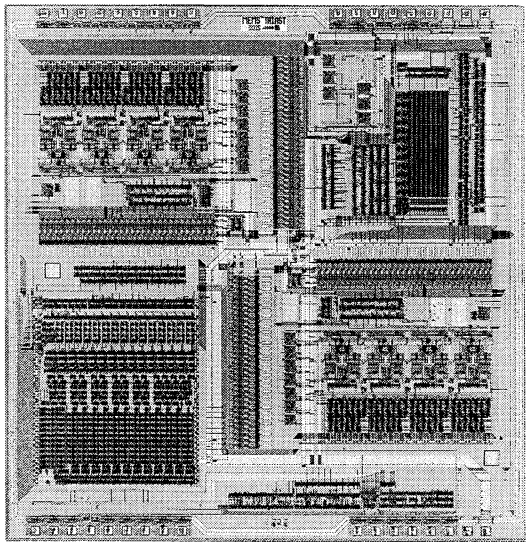

Figure 6: Photograph showing the BiAST IC chip.

2.1.3 Pressure Sensor Base and Armature

Pressure distribution data with high spatial density and large sample rates are essential to characterize flow features around hydrodynamic shapes, such as submarine control surfaces, propulsor and hull, adaptive surfaces, and others. Similar to the other sensors described throughout this paper, the pressure sensors exploit the field-based (base/armature) sensing technique[1-6] and a technique called the "block approach", where bulk micro-machined elements such as pressure-sensing diaphragms or proof masses are joined (in multiple layers, if necessary) to conventionally fabricated VLSI CMOS IC chips to form complete transducers.

Figure 7 shows a micrograph of a typical pressure sensing CMOS IC chip (base) and pressure-sensing diaphragm (armature). Each base IC chip (2.2 x 4.4 x 0.5 mm) features: (1) a differential pair of field-based sensors, along with one detector pad located toward the center of the diaphragm (maximum deflection area) and one located at a corner (reference sensor) to minimize temperature effects and variation in the assembly gap, (2) a contact and bonding aluminum frame to which the sensing diaphragm is attached, (3) a 5-pole Chebychev switched-capacitance low-pass filter, and (4) multiplexing and bus driver electronics. In principle, an array of detectors, located on the base, could be used to enhance resolution and to respond to the mechanical dynamics of the membrane.

Pressure sensors developed to date have been tailored to operate over the range from 0 to approximately 3 atm. and have a spectral noise density of approximately 1.5 $Pa/Hz^{1/2}$ (i.e., approx. 10 bits of dynamic range for the slow pressure sensor). Shock tube tests have demonstrated the capability of the devices to accurately monitor transient pressure variations with characteristic frequencies above 20,000 Hz. In practice, the diaphragm may be designed to adjust the dynamic range as dictated by the application. Enhanced pressure resolution could also be achieved by replacing the synchronously demodulated field-based sensor, used in the current device, by the charge-integrating amplifier developed for the UAST and the BiAST.

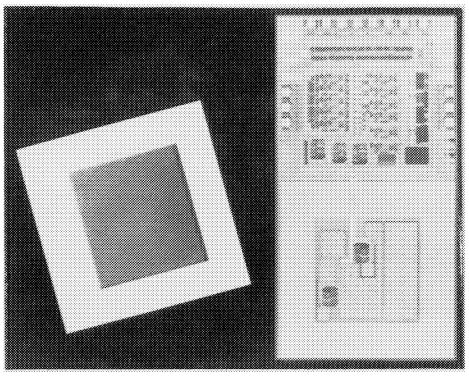

Figure 7: Microphotograph showing the pressure sensor CMOS IC chip and the silicon diaphragm.

2.1.4 Multi-Axis Strain Transducer Base and Armature

Another example of a new device that is made possible by using the approach outlined in this paper is schematically illustrated in Fig. 8. In this device the armature (emitter) contains a cross-shape structure as well as four large field emitting pads located at the corners of the armature. This armature is separated from the base by a mechanical suspension that allows it to translate and rotate in space relative to the base according to prescribed mechanical constraints. The field detector array integrated into the base is configured such that the four outermost detectors are sensitive to vertical displacement of the armature thereby providing information about vertical separation as well as pan and tilt of the armature with respect to the base. Eight additional detectors are configured to form differential pairs which are sensitive to translation of the emitter with respect to the base plane but are largely insensitive to changes in vertical separation between the armature and the base. When combined together the information provided by these detectors allows us to track the 6 DOF describing the translation and rotation of the armature with respect to base. The armature and base used to fabricate 6 DOF force/moment sensors and drag element fluid flow sensors are shown in Fig. 8.

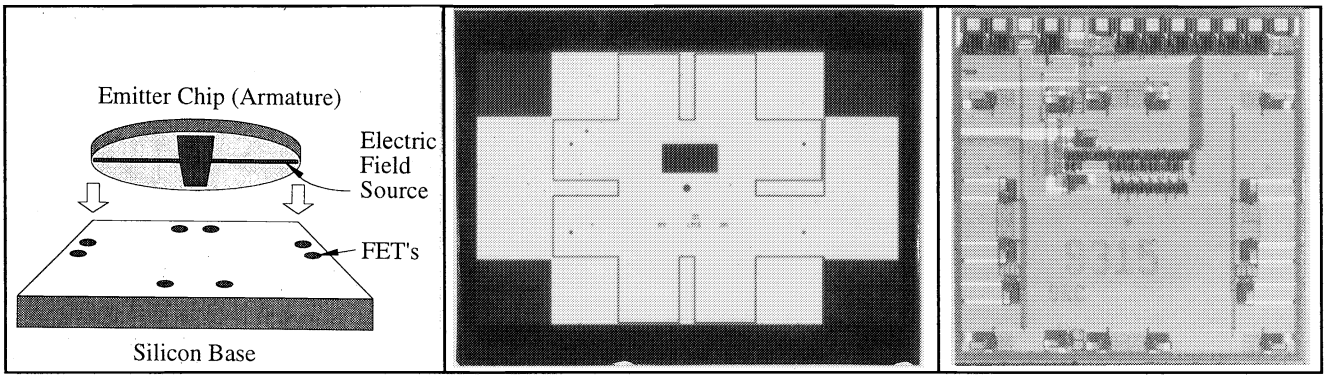

Figure 8: (Left) Schematic representation of a field-based 6 DOF sensor. The 4 outermost detectors are sensitive to vertical displacement as well as pan and tilt. Four additional differential detectors are used to measure in-plane translation and rotation about the vertical axis. The photographs show the armature (center) and the CMOS IC chip (right) used in such devices.

2.2 Packaging

Packaging of MEMS sensor devices for real world applications can, and usually does, become a formidable task. For example, the low cost fabrication advantages of an actual MEMS transducer can easily be dwarfed by the cost of packaging it in order to meet stringent requirements for protection against moisture, vibration, shock, dust, ambient pressures and temperatures, and so on. The UAST and BiAST sensor chips have additional requirements for transducing substrate strain into mechanical displacement between the emitter and IC chip internal to the package (note here that the UAST and BiAST are really micro linear extensometers and not strain gages since relative displacement, not material distortion, is used to generate a change in device output).

2.2.1 UAST package

Figure 9 (a) shows two UAST prototype packages, one which "suspends" the emitter above the IC chip and one which places the emitter in direct contact with the IC chip. Both package designs include three mounting pads on the housing's bottom side. Two pads are static and one is movable via a double flexure suspension which is connected to a link which moves the armature over the base. The primary function of these packages is to be attached to the structure to be monitored, and pass strain displacements from the third attachment pad (the front end) to the armature which position is computed by the base. Figure 9 (b) shows a photo of the direct-contact version with dimensions of 12 x 13.5 x 2.5 mm. The package material is

heat-treated beryllium-copper and the emitter support arm is assembled by a soldering process. The package also contains four capacitors, mounted to the Kapton® circuit board, which provide the filtering required for the base chip operation. The armature operates in direct contact with the base chip and is supported by a bearing surface which provides a clearance gap of approximately 2 to 5 μm between the emitter and detector arrays. Although contact friction causes some hysteresis, resolution is sufficient to monitor strains down to 0.35 micro-strain (3.5 nm at 10 mm gage length) with high bandwidth and dynamic range (11,000 micro-strain). Additionally, some UAST applications have special requirements for electrical performance and communication interfaces. For example, Fig. 9 (c) shows a number of UAST devices which have been internally hybridized with an RS-485 transceiver, EEPROM, voltage regulator, and random-addressable communication ASIC, all in bare die form.

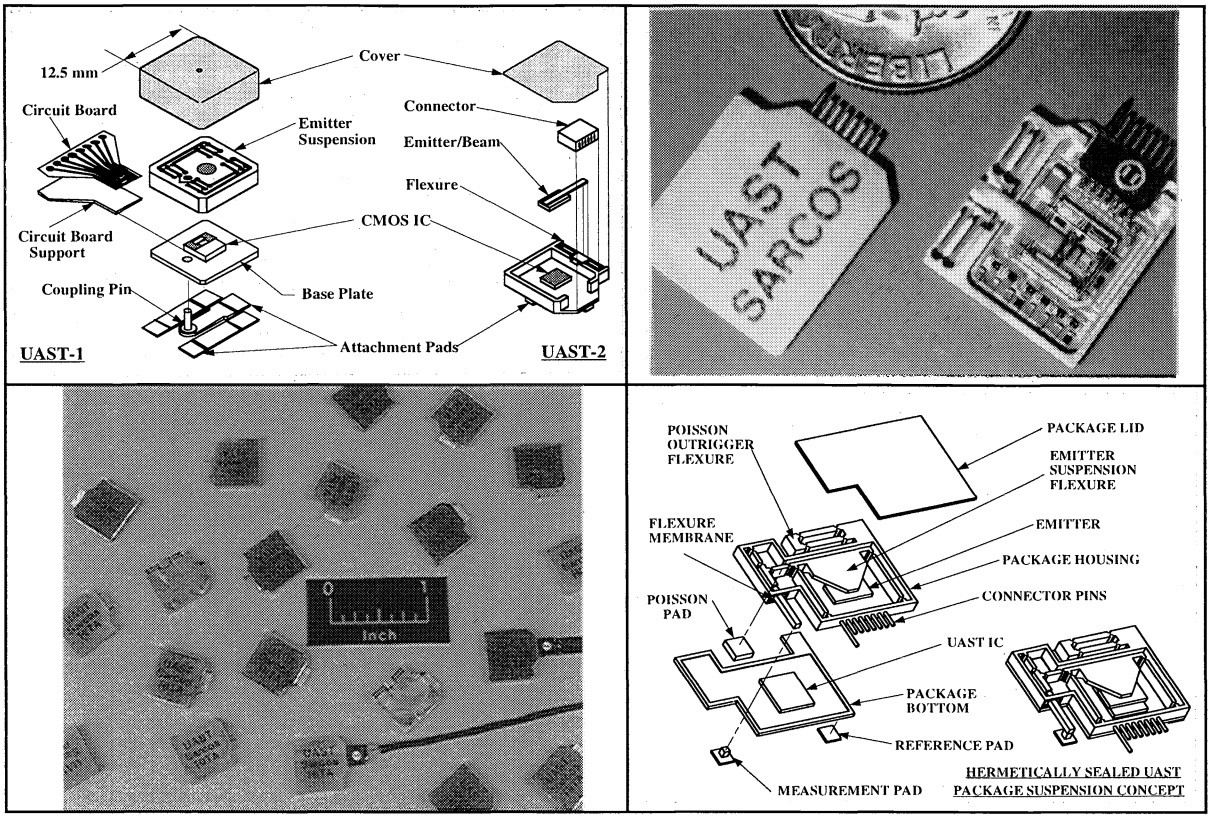

Figure 9: UAST packaging approaches showing (a) prototype versions of packages with suspended and direct-contact emitters, (b) photo of the direct-contact emitter prototype package, (c) prototype UAST packages with internally hybridized circuit elements to provide random addressable RS-485 communication, and (d) an early concept for a hermetically sealed UAST with integral flexural membrane and non-constraining outrigger foot.

2.2.2 BiAST package

The prototype UAST packages discussed above are not hermetically sealed. Upcoming versions of the UAST (and BiAST), will include flexion-based, sealed packages, similar to that illustrated in Fig. 9 (d). Here, the UAST is also mounted via two base pads and a moving pad but observe that one of the base pads is suspended by a transverse flexure which isolates the measurement from Poisson-induced deflections. The moving pad is supported by a beam and flexure assembly which passes through a membrane flexure into the inside of the package. The internal link segment, together with certain other flexures, supports the quartz armature which contains the emitter array. In this design the emitter element moves over the base chip without contact. Other UAST package design concepts include use of thin-walled electroformed bellows to provide a hermetic seal without reducing suspension compliance.

Advanced submarine, ship, and aircraft configurations are routinely developed and evaluated using numerical techniques (computational fluid dynamic analyses) which often require experimental validation. Moreover, some of these configurations utilize conformal or adaptive surfaces to actively manage separation, turbulence, boundary layer development, and other features of flow. As such, distributed transducer networks are needed to detect and measure two-axes of fluid-induced shear, as well as pressure, over the surfaces of scale model and operational vehicles moving in fluid. Recent sensor package designs for both fluid shear and pressure measurements are described below.

Fluid shear transducers (FST), which are based on "direct force" measurements, are a natural extension of the CMOS sensing described in this paper. In order to minimize interaction between the fluid and sensor, as well as sensitivity to body loads such as gravity and vehicle accelerations, some kind of viscous-coupled shear disk must be supported on a stiff suspension which undergoes small translation movements and possesses high rotational stiffness for minimal cross-axis coupling. For example, using viscous coupling between the flow and a 1.8 cm diameter suspended disk, to characterize flows with local Reynolds numbers above 10,000,000, a sensor must resolve transverse forces on the order of 50 μN (0.2 Pa of shear) with a dynamic range of 0.8 N (3 kPa) and be designed to survive substantial overloads. For a suspension with a lateral stiffness of 1,300 N/m, this corresponds to resolving dimensional deflections of less than 30 Angstroms over a range several times greater than 112 μm.

Figure 10 shows the configuration of an individual UAST- or BiAST-based shear sensor, including details of the viscous shear-coupled disk, sensor housing, suspension rods which allow controlled translation of the disk and armature with low vertical deflection, welded bellows to permit relative translation motion between the disk and housing (with high rotational stiffness to prevent cross-axis coupling) while maintaining a hermetic seal between the sensor interior and the fluid environment, armature and base chip at the bottom of the housing which measure armature translation in two dimensions, and sensor receptacle (sensor/receptacle size is 19 mm dia. and 18 mm in height). The suspension facilitates a controlled spacing between the base and armature of approximately 12 μm. The system is temperature-compensated by the suspension configuration and compatibility of materials.

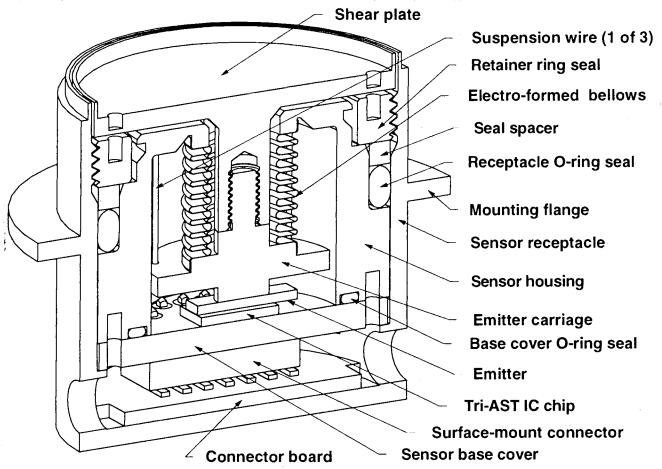

Figure 10: UAST- and BiAST-based direct-force shear sensor design presently under development.

2.2.3 Pressure sensor package

Figure 11 illustrates a hermetically sealed, flat pressure sensor package in which the sensing diaphragm is placed in direct contact with the environment and where the electrical conduits are sealed in metallic tubes in a way that is similar to that used for the shear stress sensor network described in the previous section. In the sensor package, a silicon sensing diaphragm covered with a low stress silicon nitride film is eutectically bonded to a 1-to-2 mm thick Pyrex® plate, and the latter is then eutectically bonded to a plated Kovar case. Kovar tubes are brazed on the case and act as vaults for the network electrical conduits. Electrical connection between the IC chip and the network bus is provided by a flexible Kapton® conduit which is flip-chip bonded to the IC chip. Passive electronic components, such as filter capacitors and bias resistors, are mounted on the Kapton® flexible conduit and the latter is then attached to the lid. Electrical insulation and passivation of the diaphragm and housing are provided by low stress silicon nitride (deposited on the diaphragm) and by a 15 to 25 μm thick Parylene conformal coating over the entire package. With slight modification, the pressure chip/Kapton®/Pyrex® assembly can also be integrated into a sensor housing similar to that of the shear transducer shown above such that both types of transducers can be interchanged within the same network of sensor receptacles (described later in the paper).

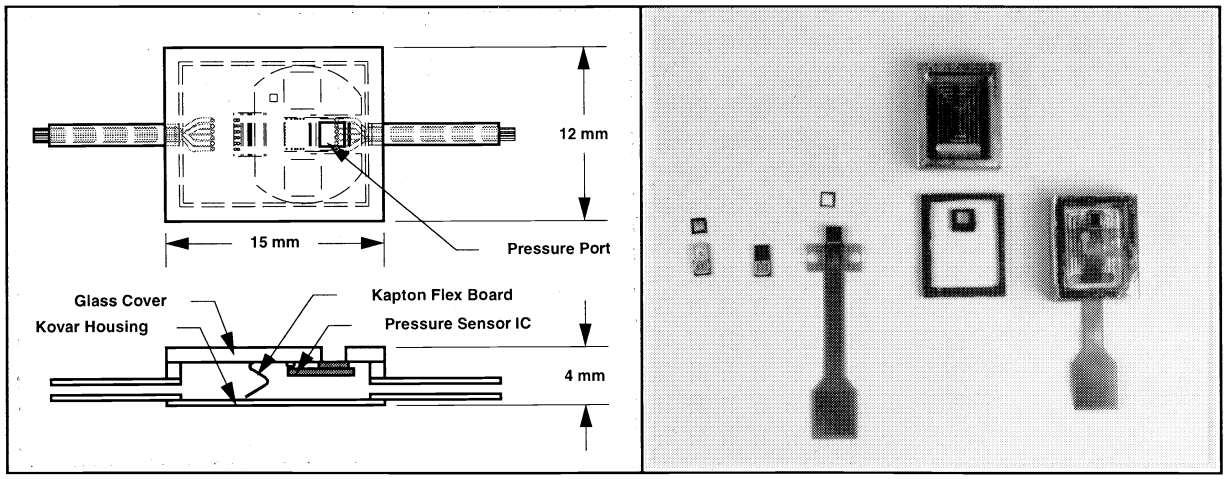

Figure 11: Schematic representation and photographs of a new pressure sensor package developed for underwater applications.

2.2.4 RDT and MAST packages

The basic elements of the RDT 2 package are shown below in Fig. 12. The components include: (1) shaft, spring-disk, and armature - which are connected in the assembled device; (2) housing with bearing tube and electrical connectors; and (3) base chip which gets bonded to the housing and contains a 1 mm diameter hole for shaft pass-through. It is important to note that all electronic elements required for the operation of the sensor are fabricated as part of the base chip. The armature (rotor disk) and base IC chip are in direct contact at the center region of the base chip, where a through-hole has been drilled. A flat bearing surface at the center of the base is achieved by standard IC processing, and a hard passivation layer is used as the bearing surface. A small mesa, approximately 10 μm high, is micromachined on the sapphire armature and provides a well-controlled gap between the emitter and the detector planes. At assembly, the gap between the base and the armature is filled with silicone oil to provide lubrication and to increase electrostatic coupling. The spring-disk (Fig. 12-a) is designed to be soft in the axial and tilt directions and stiff in rotation. The axial stiffness and preload of the spring are sufficient to maintain contact between the rotor disk and the base IC for acceleration at high g-levels while running. Figure 12-b shows a ruggedized industrial package which is sealed, and features a 4-wire pass-through. Figure 13 shows example of devices that can be fabricated using the 6 DOF armature/base assembly shown in Fig. 9. Fully operational force/moment sensors have been fabricated using this type of IC chip.

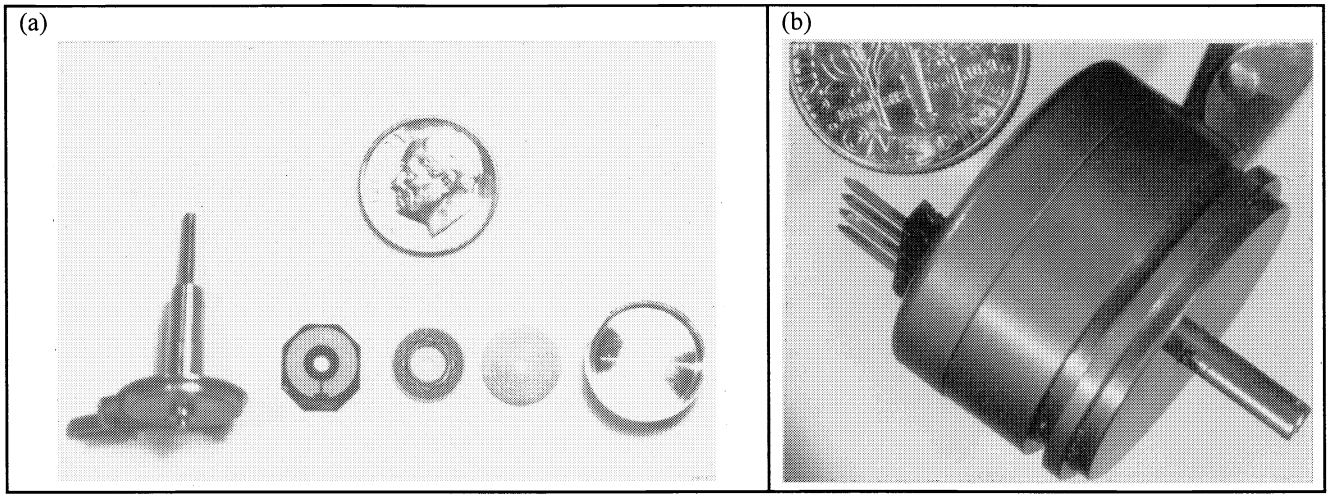

Figure 12: (a) RDT 2 package components, showing, from left to right, the rotor shaft and housing, the base IC chip, the armature (rotor disk), the disk spring, and the housing cover; (b) Industrial RDT package.

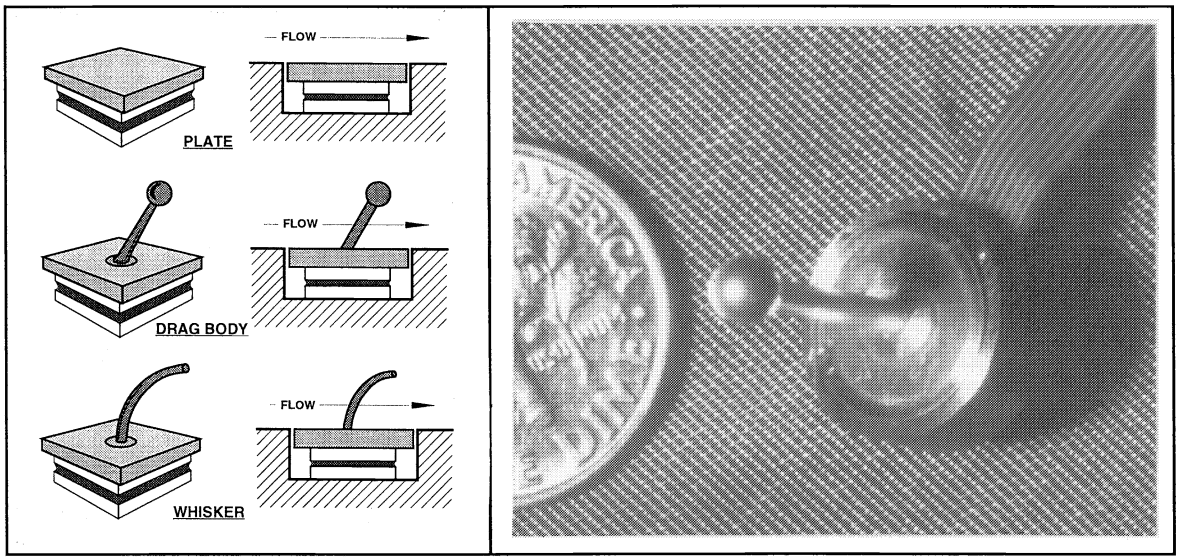

Figure 13: Schematic representation of floating element and drag element flow sensor developed using the IC chip shown in Fig. 9 (left) and photograph showing an actual device assembled using this IC chip (right).

2.3 Sensor Network Architecture and Communication Protocol

Several sensor network architectures have evolved over the last few years as each type of sensor device has been developed. One of the first schemas for communicating with a string of sensors came about with the advent of the RDT. The RDT was designed to allow multiplexing of up to 128 sensors on a three-wire bus. The first wire provides power and data, the second wire provides reset, address increment and data-clock, and the third wire is the ground return. Each RDT contains an address register determined by wirebonds on seven pads of the base chip shown in Fig. 1. A pulse train from the bus first resets the entire network and then counts the register until a comparison is achieved at each RDT. When the comparison register agrees with the sequential address, a 16-bit serial data stream is impressed on the data line.

More recently, to meet the goals of low cost and high performance for sensor networks requiring literally thousands of channels (e.g., instrumenting a model submarine for hydrodynamic flow characterization), a data acquisition system has been developed based on a Pentium PC utilizing on-board RAM as a large data buffer. After completion of a data acquisition sequence (limited by the capacity of on-board RAM), the contents of the RAM are transferred to the PC's hard drive. This approach supports a higher data transmission rate (in excess of 40 Mbits/sec using the Pentium's PCI bus) than is possible with sustained writing to a hard drive (e.g., past efforts under DARPA's ISNP and SNAP projects realized a practical limit of approx. 12 Mbits/sec in writing data to a hard drive using a VME bus architecture). The only drawback to this approach is the finite limit to the amount of data which can be acquired before requiring a pause in testing activities to write data to the hard drive. However, recent price drops in PC's and RAM make this approach attractive. Of course, for active control system applications, storing of acquired data may not be necessary.

The general approach for implementing the PC-based data acquisition system is shown in Fig. 14 with sample rate calculations and estimated test duration for a single string of sensors. This system approach can be optimized by recognizing the two principal bottlenecks of data transmission: 1) the 2.5 Mbits/sec limit on any given string of sensors (each data bit requires four clock cycles to send or receive) and 2) the approx. 40 Mbits/sec (5 Mbytes/sec) limit on sending data over the PCI bus to the system RAM. Since there are four PCI card slots on the Pentium PCs under consideration, this architecture should be able to support up to 16 sensor strings (at 4 strings per card) per PC-based data acquisition system. Likewise, with 256 Mbytes of RAM and 16 strings of fully populated sensors, this network architecture could support a minimum of 51 seconds of data acquisition (or 76.5 seconds with 384 Mbytes of RAM). The system uses a serial bus protocol (described in more detail below), supporting up to hundreds of sensors on a 6 wire bus: 5V power, 10MHzClk, Token, Data+, Data-, and Ground. The bus uses a modified Token Passing scheme (described in the next section), where the "address" of a particular sensor is implied by its physical order on the bus, making any sensors on the bus interchangeable. The master controller for the bus is housed on a PC plugin card, and drives a variable number of sensors. The protocol is synchronous with a 10MHzClk which is distributed to all sensors on the bus, and eliminates the need for each sensor having a local stable oscillator, such as a clock crystal.

There are several means to transmit data down the bus, depending on the length of wires, the number of sensor devices, and the presence of noise sources from the environment. Figure 15 shows three options for data transmission, including a single data line, differential data lines using line drivers residing on the CMOS sensor IC chips, and differential data lines using RS-485 transmitters hybridized within the sensors. The differential data line approaches are preferred due to the substantial improvement in noise immunity during operation. All three approaches have been successfully demonstrated.

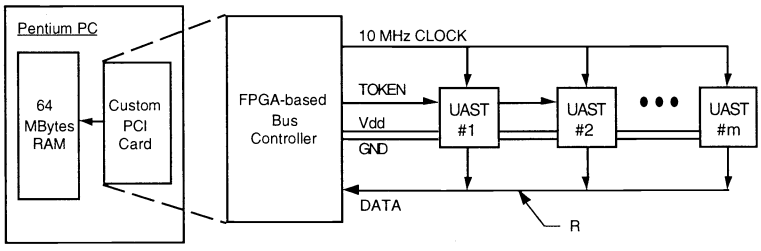

CLOCK -- 10 MHz nominal
TOKEN -- sample rate, up to 50 kHz, limited by A/D, ability to encode sensor configuration
n -- number of sensors, 1 to 256.
RØ -- data rate; 2.5 Mbits/sec (max. burst rate)
rate -- sensor sample rate (samples per second)
R1 -- average data rate to the PC in bytes/sec

- R1= 18 * n * rate < RØ (= 2.5 x 10^6 max.)
- e.g., 277 sensors @ 500 Hz, 138 @ 1000 Hz, etc.

Figure 14: Pentium PC-based token-passing sensor network architecture with sample rate calculations and estimated run times based on available RAM.

The need for communication with literally thousands of sensors on a given network of this type requires 1) the capability for high data transmission rates (using a distributed 10 MHz clock, the protocol described in the next section supports 2.5 Mbits/second per sensor string, i.e., 4 clocks per data bit), 2) the synchronous sampling of data amongst all sensors on a given string (the rising edge of token is propagated down each sensor string with less than an estimated 10 nano-second delay per sensor, e.g., 100 sensors will synchronously latch their respective data on a given string to within 1 micro-second of each

other), and 3) the ability to re-configure various types of sensors on a given string within that network, between data runs. Thus, the sensor-network communication interface is required to be the same for all devices on this type of network bus. Each device must use the same 18-bit data format (consisting of a start bit, fifteen data bits, a parity bit, and a stop bit, all transmitted at four clocks per bit), the same token-passing protocol, and run from the same distributed 10 MHz clock and supply voltage. All of these capabilities are integrated on the UAST and BiAST IC chips.

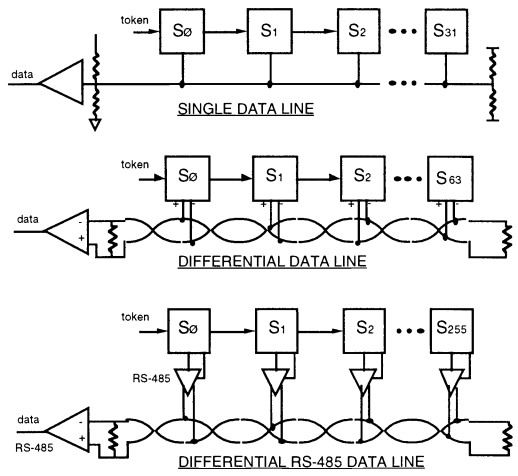

*significantly longer bus lengths may be achievable, depending on application

Single Data Line:
- for short runs with low noise
- both ends terminated
- max length = 3 meters*
- max. # of sensors = 32
- A total of 5 conductors (one less than below)

Differential Data Line:
- for moderate runs w/ noise
- both ends terminated
- max. length = 5 meters*
- max. # of sensors = 64
- drivers included on sensor ASIC
- A total of 6 conductors

Differential RS-485 Data Line:
- for long runs with noise
- both ends terminated
- sensors require RS-485 T/R die
- e.g., 10 meters with 256 sensors* or 30 meters with 32 sensors* (based on 100-165pF/m wire capacitance and 5 pF/sensor)
- A total of 6 conductors

Figure 15: Schematic representation of representative sensor network data transmission line options. Data bus options utilizing a network with distributed clock, Vdd, Gnd, and Token.

There has also been the need to interface other devices, such as pressure transducers and accelerometers, with this network architecture. To this end, an application specific integrated circuit (ASIC) has been developed for Newport News Shipbuilding (NNS), as shown in Fig. 16. The NNS ASIC is a custom CMOS IC used to interface Sarcos pressure sensors or other analog output sensors to the NNS serial bus containing UASTs and BiASTs. The NNS ASIC chip is mounted with a Burr-Brown ADS7817 12 bit A/D MSOP, an Analog Devices AD580 voltage reference chip, an 78L05 voltage regulator chip, and the Sarcos ISNP pressure sensor in a hybrid watertight package. Sensors on this network bus can be any combinations of BiASTs, and hybrids containing NNS ASIC chips combined with pressure sensors or accelerometers.

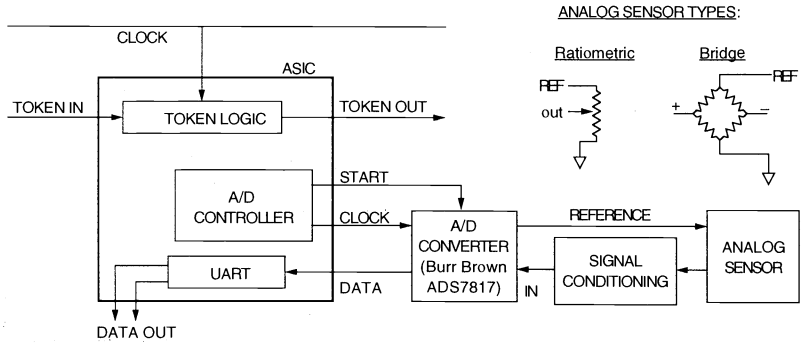

Figure 16: An ASIC compatible with available analog-to-digital allows us to interface various types of analog sensors with the UAST digital bus architecture.

The master controller can send one of two different messages to the first sensor; one used to initiate periodic sampling of the entire network of sensors (sample), the other for transmitting configuration messages to a selected "type" of sensor on the network. Both types of messages begin with a "low-to-high" transition on the Token line going from the master controller to the first sensor in the network. When a sensor detects a rising-edge on its TokenIn pin it needs to determine whether it is a sample or configuration message. A sample message is a low-to-high transition on the TokenIn line, remaining "high" for at least 10 clocks, while a configuration message starts by going "high" for 4 clocks and then "low" for either 4 or 8 clocks, then "high" for either 4 or 8 clocks, etc. The configuration message is encoded onto the Token by the master controller, and is repeated by every sensor on the bus to its downstream neighbor. The configuration message is sent at a rate of 1.25 Mbps, or 8 clocks per bit and consists of a "start" bit(0), 4 "type" bits, and 12 configuration bits. In this way, the schema supports 16 different "types" of sensors, such as UASTs, BiASTs, and pressure sensors. The device "type" bits have been subdivided into four blocks of four, with each block reserved for a particular kind of device. So, addresses from 0 - 3 are allocated to the BiAST, 4 - 7 are allocated to the UAST, 8 - 11 are allocated to the NNS-ASIC, and 12 - 15 are presently unallocated. Each chip has two bond pads which can be strapped high or low to set the full address of that device.

Information bits in the configuration messages can be used for a variety of purposes, depending on how each sensor is designed. For example, the pressure sensors for the above project can be configured with an anti-alias filter rolloff INDEPENDENT of the sample rate. Likewise, the shear sensors can be configured to report one, two, or all three axes of force with either buffered or unbuffered data. As yet another example, intrinsic to the operation of a UAST sensor network is the flexibility to trade sensor sample rate against UAST strain resolution, i.e., using fewer clock pulses to convert the detector values, speeds up the calculation of the strain value but with a corresponding decrease in strain resolution. The number of

sensors on the network also impacts the sample rate since more sensors require more time to transmit their data which occurs at 2.5 Mbits/sec. For example, 128 sensors operated in 15-bit mode (resolution of 0.35 micro-strain, i.e., 3.5 nm) can be sampled at 131 Hz each, while 10-bit mode (11.25 micro-strain resolution) allows sampling at 786 Hz each. Likewise, a smaller number of 8 sensors can be operated in 15-bit and 10-bit modes while sampling at 148 Hz and 2452 Hz, respectively. It is also conceivable that future sensors could be configured to report data only at specified intervals, allowing interleaving of data samples between different groups of sensors with different sample rates, all on the same string. The configuration field allows for up to 4096 different combinations with the message taking 18 x 8 bits, or 14.4 μs.

In all cases, transitions on the TokenIn pin occurring after a period of inactivity (TokenIn "low") are passed through the ASIC to the TokenOut pin with a minimal 5-10 nsec propagation delay. The TokenIn signal is sampled by the rising edges on the 10MHzClk line, so a Token edge can propagate through 10-20 sensors before the cumulative delay causes the edge to slip to the next 100ns clock cycle. This has no effect on configuration messages; sample messages will be delayed in multiples of 100ns (the period of 10MHz clock) for each subsequent "clump" of 10-20 sensors. This allows a sample message to be passed all the way to the end of a hundred sensor bus within 1μs.

"One-to-zero" transitions occurring after the TokenIn pin has been "high" for more than 10 clocks are delayed by a fixed number of clocks before being passed out the TokenOut pin. This delay allows the sensor to send its data message on the differential data lines. The message sent by each sensor consists of 18 bits, each lasting 4 clock cycles (400ns), making the fixed delay from TokenIn to TokenOut 7.2us. The 18 bits (generating a bit stream at 2.5 Mbits/s) in the data message are: Start bit(1), 15 data Bits, Parity bit (odd parity of the 15 data bits), and a Stop bit(0). Each sensor can send back two types of data messages, depending on if it is responding to a configure or sample message. The data message elicited by a configuration message is a playback of the 12 configuration bits plus three other bits. In the NNS ASIC, these come from three I/O pins on the ASIC. In the BiAST, they report internal status information. The data message elicited by a sample message is the sampled data. In the NNS ASIC, 12 bits come from the A/D converter, and the other three come from I/O pins on the ASIC. In the BiAST, all 15 data bits come from strain readings. BiASTs can respond with one, two or three data messages, depending on how they are configured.

A configuration message is contrasted by the string-wide sample data message which is recognized by each sensor when the token line rises and remains high for at least 10 clocks (all sensors subsequently sample data on the 11th clock). One useful feature of the protocol is that after a configuration message is sent for ANY of the sensor types, ALL sensors of ALL types on the string report back their configurations for confirmation. Thus, seven different types of sensors on a string would require seven different configuration messages to begin operation; subsequent reconfiguration of a single group (type) of sensors would require only one configuration message but all sensors (representing seven different types) would reconfirm their configuration status.

3. CURRENT APPLICATIONS

UAST sensors and associated network technology are already under evaluation for monitoring loads in common aircraft, as well as for instrumenting a variety of test structures. One opportunity which presented itself was to evaluate UAST network performance during dynamic testing of a 1/2-scale F/A-18 vertical tail torque box at Boeing's test facility in St. Louis. Based on finite element analysis of stress distributions, four UASTs were bonded to specific locations on one of the 40 inch tall 0.125" thick skins, as shown in Fig. 17. Data from the digital sensors were collected and comparisons of the response with conventional foil strain gages were compiled. The tail was exposed to moving base excitation in both sinusoidal sweeps and band-limited random inputs. The frequency band of interest was 5-150 Hz, the first two primary modes of the tail being in this range. The digital sensors were also successfully used to provide input to a neural network-based algorithm using piezoelectric patches as actuators to actively control the first two vibration modes of the model.

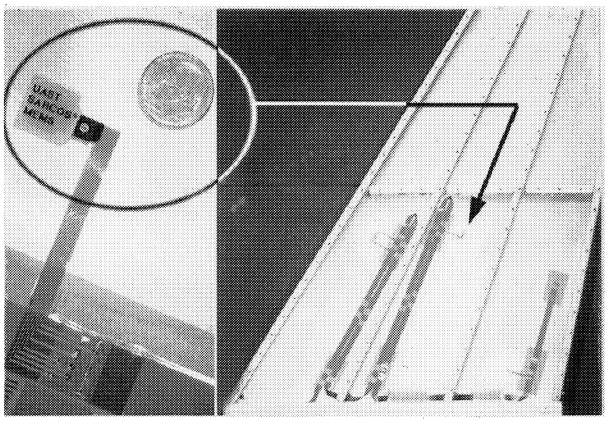

Figure 17 -- Installation of a network of 4 UAST sensors on a 1/2-Scale F/A-18 vertical tail torque box using a flexible flat ribbon bus with connectors.

The flexible polyimide bus developed for this effort utilizes intermittent ground traces and a backing foil to promote shielding of clock, data, and power lines from potentially strong noise sources, such as those found on operational aircraft. A seven pin "nano-series" connector from Omnetics was adopted for the 0 and 90 degree orientation "pigtails" to promote ease of installation and removal of sensors from the bus. The figure shows the bus configuration and layout utilized to install the sensor network into the torque box test article. The UAST's on-chip differential line drivers were demonstrated to be capable

of transmitting data down a 30 foot length of this bus configuration (longer lengths should be possible) and the 10 MHz clock was successfully distributed over the same length using a Pericom driver and appropriate bus termination design practices. Some applications have utilized a much simpler 6-wire (twisted pairs) round cable approach for the bus.

Another application for UAST sensor networks is in health usage and monitoring systems (HUMS) for rotorcraft. Figure 18 shows installation of eight UASTs on a UH-60 Blackhawk rotor hub assembly as part of the NASA/ARMY Rotorcraft Aircrew Systems Concepts Airborne Laboratory (RASCAL) HUMS development effort. In addition to monitoring in-flight loads to provide an aircraft-specific flight loads history, these sensors will also be part of a pilot-cueing system to provide tactile feedback of airframe and rotor loads to the pilot during maneuvering. These devices have been hybridized with internal electronics to make them compatible with a random-addressable RS-485-compliant bi-directional communication protocol. The principal attributes of the system include all-digital operation to reduce wiring requirements and installation costs, and greatly reduced requirements for periodic calibration due to the UAST's zero-drift absolute encoding of strain.

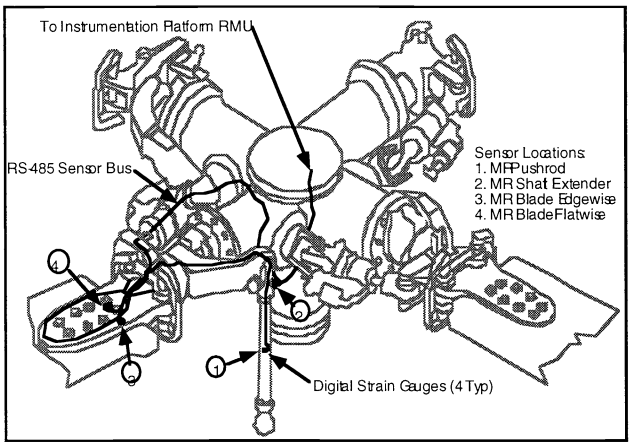

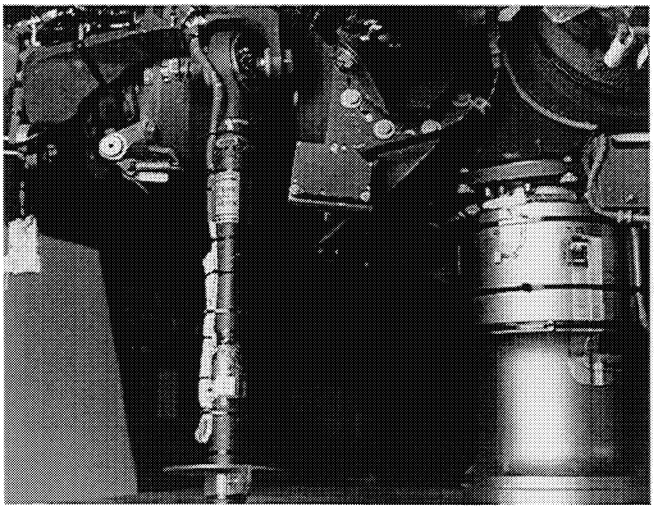

Figure 18: Installation of eight random-addressable, RS-485-compliant hybrid UASTs on a UH-60 Blackhawk rotor hub assembly as part of the NASA/ARMY Rotorcraft Aircrew Systems Concepts Airborne Laboratory (RASCAL) HUMS development effort.

In another application arena, hydrodynamic and hydroacoustic design/analysis tools are required to achieve a computationally-based design capability for submarines in the areas of resistance, hydroacoustics, and maneuvering. Validation of these tools is an integral part of their successful implementation. As such, an instrumentation technology approach is required which can provide high resolution measurements of surface pressure and shear stress along the hull, sail, propulsor blades, and/or control surfaces of experimental models. The challenge in making these measurements is obtaining sufficient spatial and temporal resolution to provide meaningful data to the computational fluid dynamicists, and at an affordable cost per channel.

For example, Fig. 19 shows a network of pressure and vibration sensors integrated on both faces of a prototype 1/4- scale propulsor blade section. This early network architecture consists of 72 sensors housed in 56 hermetic packages designed for use in different environments. More specifically, the network is divided into two major branches, installed on opposite faces of the blade and comprised of: (1) 8 nodes which perform analog-to-digital conversion and transmit data over a digital bus at a combined rate of 12 Mbits/sec; (2) 8 high-speed pressure sensors (sampled at 50 kHz); (3) 32 low speed-sensors (sampled at 5 kHz); and (4) 32 collocated pressure and vibration sensors (also sampled at 5 kHz). The CMOS base/armature concept outlined throughout this paper was readily combined with bulk silicon micro-machining techniques and better-than-hermetic bonding methods to fabricate the sensors used in this example. The accelerometer readings were used to compensate for vibration-induced pressure fluctuations (e.g. blade flutter and other mechanical disturbances).

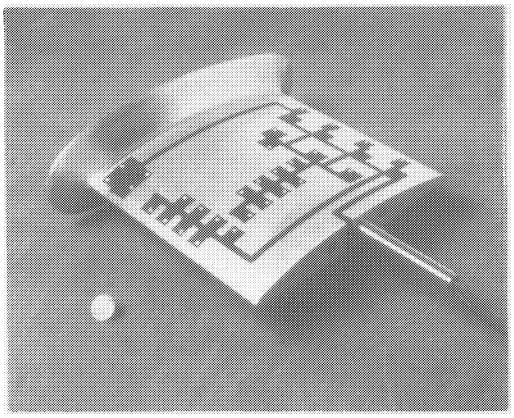

Figure 19: Propulsor test blade showing the layout of the pressure and vibration sensor network.

More recently, an instrumentation technology development effort, entitled "Instrumentation for Integrated Design Practices" (I2DP), has been undertaken to develop a universal sensor network

architecture along with a suite of sensor types (e.g., pressure, shear, vibration, sound, etc.) suitable for installation on a variety of test vehicles. The specific short term objective of project activities has been to provide high fidelity surface pressure and shear stress measurements on advanced sail designs configured for existing 1/16th- and 1/4-scale operational submarine test models. The benefits of I2DP technology development will be the generation of experimental results on a variety of test platforms in direct support of validating computational fluid dynamic analysis tools. This should lead to opportunities for more full coverage instrumentation of the sail and/or hull on larger models where the total sensor count might exceed 4000 sensors.

Perhaps the greatest attribute of the I2DP bus and conduit architecture is the ensured flexibility in configuring each network for specific types of model vehicle test runs or as new sensors emerge (i.e., if an investment is made in installing a conduit system onto a test vehicle, it should be possible to swap out old sensors for new ones, as they are developed by Sarcos and/or other sensor vendors). Figure 20 shows a string of "vaulted" (sealed) sensors where mixed types of transducers (some are two-axis shear, others are pressure, and a thin film anemometer module is also shown). All sensors share a common sensor receptacle and network conduit interface. In addition to each sensor module being hermetically sealed, the conduit tubing and receptacles form a separate control volume which can be gas-filled and pressure compensated (via a bellows with sufficient starting volume to accommodate the anticipated increase in external water pressure) to prevent intrusion of water when operating the network at great pressures. The sensor modules utilize standardized connectors and O-ring seals to facilitate easy removal or to reconfigure the network with different combinations of sensor types for various applications. The bus will be capable of a wide range of sample-rates and numbers of sensors (of multiple types on each string, if desired). For example, a single 20 foot long string could be populated with 128 sensors sampled at 1000 Hz. Note also that vendor-specific plug-in modules can be developed to interface more conventional sensor types (e.g., hot film anamometers, accelerometers, or others) with the digital bus on an as-needed basis.

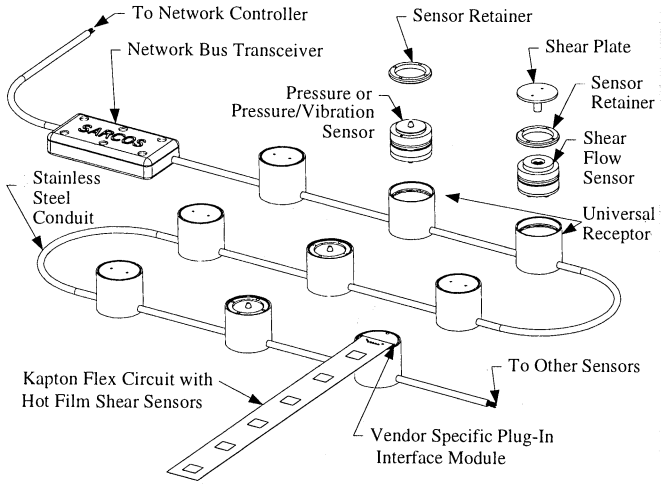

Figure 20: Network configurability is obtained by using a standardized bus and conduit architecture. Shown are two-axis flush mounted flow sensors and pressure sensors, along with a hot film anemometer to show how vendor-specific application modules can be employed.

4. UPCOMING APPLICATIONS AND CONCLUSIONS

Sarcos' MEMS sensor network development effort was initiated in response to problems encountered with the reliability of wiring harnesses, as well as the high cost of sensors required for complex machines such as high performance telerobots (e.g., Fig. 21). The promises of achieving unprecedented performance in smart structures such as adaptive hydrodynamic surfaces and the entire area of condition based maintenance and operation soon led to a rapid extension of the original class of internal machine state sensors (RDT, UAST, MAST) to include a new class of devices that are well suited to monitor the environment in which the system operates (e.g. pressure, vibration and sound).

As indicated in the previous section devices such as the UAST, BiAST, pressure sensor networks are now being fielded. It is anticipated that our initial targets, namely the RDT and the MAST, will likewise find their way into the above application arenas in the near future.

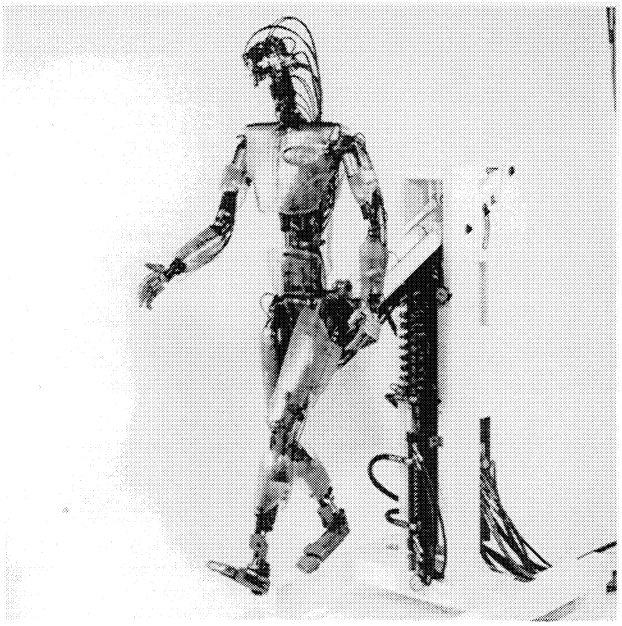

Fig. 21: Anthropomorphic hydraulic robot.

ACKNOWLEDGMENTS

The authors gratefully acknowledge the direct contributions from D.P. Marceau, D.L. Wells, F.L. Williams C.C. Davis, D.G. Petelenz, and D. Beutel. The authors also gratefully acknowledge support for this effort by the Defense Advanced Research Projects Agency under contract numbers: F33615-87-C-5267, N00014-93-C-0112, N00014-96-C-0345, DAAH01-95-C-R144, DABT63-95-C-0033, N00014-93-C-0181, DABT63-98-C-0048, from NAVSEA under Newport News Shipbuilding (N00024-95-C-2102) as well as with DARPA and NASA funded projects from Lockheed Martin and The Boeing Company.

REFERENCES

1. B.J. Maclean, M.G. Mladejovsky, M.R. Whitaker, M. Olivier and S.C. Jacobsen, *A Digital MEMS-Based Strain Gage for Structural Health Monitoring*, in Nondestructive Characterization of Materials in Aging Systems, Vol. 503, Proceedings of Material Research Society Symposium, Boston, MA, Dec. 1-5 (1997).
2. S.C. Jacobsen, M.Olivier, B.J. Maclean, M.G. Mladejovsky and M.R. Whitaker, *Multi-Regime Integrated Transducer Networks*, Solid-State Sensor and Actuator Workshop, Hilton Head Island, South Carolina, June 8-11, 1998.
3. S.C. Jacobsen, et. al., *Field-based Microsystems for Strain Measurement*, Proc. ASME Winter Annual Meeting, November, Chicago, IL (1988).
4. S.C. Jacobsen, et. al. *Displacement Sensing by Direct Mechanical Modulation of Shaped Electro-Active Micro-Structures*, Proc. IEEE Micro-Electro Mechanical Systems Workshop, Feb. 11-14, Napa Valley, CA (1990).
5. S.C. Jacobsen, et. al., *Field-Based State Sensing in Micro-Motion Systems*, in Integrated Micro-Motion Systems - Micromachining, Control, and Applications, F. Harashima, Ed., Elsevier Science Publishers (1990).
6. S.C. Jacobsen, et. al., *Advanced Intelligent Mechanical Sensors (AIMS),* Proc. IEEE Transducers '91, June 24-28, San Francisco, CA (1991).